Available online at www.sciencedirect.com
SCIENCE DIRECT®
International Journal of Mass Spectrometry 228 (2003) 349–358
International Journal of Mass Spectrometry
www.elsevier.com/locate/ijms

Gas-phase basicity and enantiodiscrimination of some phosphorous-containing α-amino acid mimics

A. Paladini[a], D. Scuderi[a], A. Laganà[a], A. Giardini[a,b], A. Filippi[c], M. Speranza[c,*]

[a] *Dipartimento di Chimica, Università di Roma "La Sapienza", I-00185 Rome, Italy*
[b] *CNR-Istituto Materiali Speciali, I-85050 Tito Scalo (Pz), Italy*
[c] *Dipartimento di Chimica e Tecnologia delle Sostanze Biologicamente Attive, Università di Roma "La Sapienza", I-00185 Rome, Italy*

Received 23 October 2002; accepted 18 March 2003

Dedicated to Professor Helmut Schwarz on the occasion of his 60th birthday and in recognition of his outstanding contributions to gas-phase ion chemistry.

Abstract

The kinetic method has been used for enantiodiscriminating important chiral residues from post-translationally modified proteins, i.e., the *O*-phospho α-amino acids, and some chiral α-amino acid mimics, i.e., the α-aminophosphonic acids. Their proton affinities (PA) have been evaluated using the same method in its extended form which allows the estimate of the entropy contributions on the kinetic measurements. The kinetic approach is based on the competing collision-induced decomposition (CID) of suitable proton-bound complexes between the P-containing molecules and suitable reference compounds, e.g., α-amino acids. The investigation was carried out in a QqQ instrument as a function of the collision energy (4–14 eV). The proton-bound complexes were generated in an electrospray ionization (ESI) source from calibrated water/methanol solutions of the two components. The experimental results have been discussed and compared with theoretical calculations.

Keywords: α-Aminophosphonic acids; *O*-Phospho α-amino acids; Gas-phase enantioselectivity; Proton affinity; Mass spectrometry

1. Introduction

The key role of α-amino acids in the chemistry of life and as structural units in peptides and proteins has led to intense interest in the chemistry and biology of their mimics. An important class of such mimics are the α-aminophosphonic acids, which are analogues of α-amino acids in which the carboxylic group is replaced by a phosphonic function [1]. These compounds are extremely important antimetabolites, which may efficiently compete with their carboxylic counterparts for the active sites of enzymes and other cell receptors. However, the replacement of the carboxylic functionality with the phosphonic one has a number of important consequences as regards to the structure and the acid/base properties of this family of α-amino acid mimics which deserve careful investigation.

The same considerations apply to another family of P-containing molecules, such as phosphorylated

* Corresponding author. Tel.: +39-064-991-3497; fax: +39-064-991-3602.
E-mail address: maurizio.speranza@uniromal.it (M. Speranza).

1387-3806/$ – see front matter
doi:10.1016/S1387-3806(03)00129-5

α-amino acids. Reversible protein phosphorylation is involved in a multitude of regulatory mechanisms for the control of intracellular protein functionality [2–5]. Serine, threonine, and tyrosine, and a number of other amino acid residues can be modified by the attachment of a phosphate group. The physiological impact of these modifications can be better elucidated after a detailed characterization and stereochemical identification of these P-containing molecules.

$$[AH]^+ \overset{k_1}{\leftarrow} [A \cdot H \cdot ref]^+ \overset{k_2}{\rightarrow} [Href]^+ \quad (1)$$

These tasks can be conveniently fulfilled through the application of Cook's kinetic method, based upon the generation of the cluster ions $[A{\cdot}H{\cdot}ref]^+$ of Eq. (1), where A is the P-containing molecule and ref is a suitable reference compound, in an electrospray ionization (ESI) source [6] of a tandem mass spectrometer [7]. The mass-selected $[A{\cdot}H{\cdot}ref]^+$ ion is activated by collision with a suitable gas, for example N_2, and the fragments ($[AH]^+$ and $[Href]^+$ in Eq. (1)) arising from its collision-induced decomposition (CID) mass analyzed [8–12]. This method has been repeatedly used to measure the thermochemical properties of a very wide range of organic compounds and to discriminate and quantify the enantiomers of chiral molecules, including amino acids and peptides [13–19].

The standard form of the kinetic method allows quantitative determination of the gas-phase acid/base properties of A, provided that certain requirements, such as the absence of reverse activation barriers and equal entropy changes for the two dissociation channels of Eq. (1), are met [8–11]. In this frame, the $\Delta PA = PA(A) - PA(ref)$ difference is calculated from the relative abundances of the individual protonated fragments, $[AH]^+/[Href]^+$, through Eq. (2).

$$\ln \frac{k_1}{k_2} = \ln \frac{[AH]^+}{[Href]^+} = \frac{PA(A) - PA(ref)}{RT_{eff}} \quad (2)$$

Accordingly, the slope of the linear plot of $\ln([AH]^+/[Href]^+)$ vs. the proton affinity of a series of reference compounds (PA(ref)) provides an estimate of the effective temperature term (T_{eff}), whilst the *x*-intercept gives the PA(A) value.

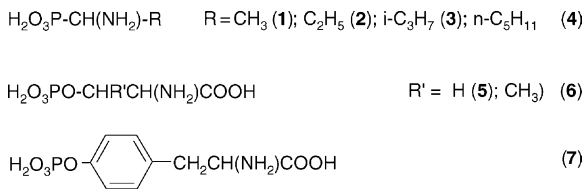

Plate 1.

The constraints for the measure of the PA affinity by the standard kinetic method are unlikely met in the case of α-aminophosphonic acids **1**–**4** and the phosphorylated α-amino acids **5**–**7** (Plate 1). Indeed, the condition of equal entropy changes (and of comparable reverse activation barriers) for the two dissociation channels of Eq. (1) is better satisfied the closest are the structures and the functional groups of the analyte A and the reference molecules (ref) and the more similar is their spatial arrangement around the proton. Unfortunately, very few phosphorylated molecules can be used as potential reference compounds, and therefore, we are obliged to take as ref the closest structural and functional analogues of A, i.e., the α-amino acids. This necessity introduces a further problem. Being the amino group of α-amino acids, the most basic site, the question arise as to whether the same group is the most basic one in **1**–**7** as well.

From the above mentioned, it follows that the experimental evaluation of the PA of **1**–**7** requires a preliminary computational assessment of their most basic site. Then, the accurate PA measurements require the use of the extended treatment of the kinetic method [12,20–23] which allows for the deconvolution of the enthalpic and the entropic contributions to the competing dissociation channels of Eq. (1). A similar kinetic procedure is employed for enantiodiscriminating the selected chiral P-containing α-amino acids.

2. Experimental

2.1. Electrospray ionization mass spectrometry

The pure (*R*)- (A_R) and (*S*)-enantiomers (A_S) of aminophosphonic acids **1**–**4** and the phosphorylated α-amino acids **5**–**7**, as well as of the reference amino

acids (ref), were obtained from Sigma–Aldrich Co. The CID experiments were performed by using a commercial API 100/300 triple-quadrupole (QqQ) mass spectrometer from Perkin-Elmer Sciex Instruments, equipped with an ESI source and a syringe pump. Operating conditions for the ESI source were as follows: spray voltage, 3.8 kV; capillary temperature, 298 K; sheath gas (N_2) flow rate, 30 units (roughly 0.75 L/min). The selected gaseous complexes were generated by electrospraying at a flow rate of 10 μL/min 50:50 water/methanol solutions containing equimolar amounts (10 μM) of the optically pure P-containing amino acid (A) and the reference amino acid (ref). The experiments were conducted in the positive ion mode. Reported spectra represent the average of about 150 scans, each requiring 0.1 s.

Ions corresponding to the mass-to-charge ratio of the proton-bound dimers $[A{\cdot}H{\cdot}ref]^+$ were mass selected using the first quadrupole Q. Collisional activation of the dimers was achieved in the second "rf-only" quadrupole q at laboratory collision energies ranging from nominal 4 to 10 eV, using a N_2 target at pressures (pressure ca. 10 mbar) corresponding to single collision conditions (i.e., primary ion beam attenuated by <20%) [24]. The CID fragments were eventually analyzed in the third quadrupole Q of the instrument.

The same procedure has been employed to analyze the CID fragmentation of the diastereomeric proton-bound trimeric ions $[A_S{\cdot}H{\cdot}(ref)_2]^+$ and $[A_R{\cdot}H{\cdot}(ref)_2]^+$ (laboratory collision energies from 4 to 14 eV), using reference compounds of defined configuration.

2.2. Computational details

Quantum-chemical calculations were performed using the Gaussian 98 sets of programs [25]. The 6-31G* basis set was employed using the B3LYP hybrid density functional procedure [26]. At the same level of theory, frequency calculations were performed for all optimized structures to ascertain their minimum nature. Thermal contribution to enthalpy at 298 K and 1 atm, which includes the effects of translational, rotation, and vibration, was evaluated by classical statistical thermodynamics with the approximation of ideal gas, rigid rotor, and harmonic oscillator behavior and using the recommended scale factors (0.98) for frequencies and zero point energy corrections [27].

3. Results and discussion

3.1. The site of protonation

A preliminary aspect to be considered before applying the extended kinetic method to the measure of the PA of both the α-aminophosphonic acids **1**–**4** and the phosphorylated α-amino acids **5**–**7** concerns their most basic site. Some insights into this point were obtained by extensive quantum-mechanical calculations on protonated **1** and **5**, i.e., the simplest members of two families of compounds, at the B3LYP/6-31G* level of theory. Exploration of the potential energy surfaces (PES) of protonated **1** and **5** led to the location of several different critical points, unambiguously characterized as true minima by analytical computation of the corresponding vibrational frequencies. The connectivity and the main geometrical parameters of these molecules and their protonated ions are shown in Fig. 1. The absolute and relative energies of the relevant critical structures are reported in Table 1.

Ion **I**, formally obtained by protonating the nitrogen atom of **1**, is the global minimum on protonated **1**'s PES. Its optimized geometrical parameters, in particular the pronounced P=O···H–N coplanarity (dihedral angle: 6.1°; O···H–N angle: 121.8°), coupled with the distorted C–P=O (106.5°) and P–C–N angles (103.1°), relative to the corresponding ones in **1** (118.8 and 105.9°, respectively), reveal the occurrence of an intramolecular P=O···H–N electrostatic interaction (O···H distance: 2.04 Å). A similar intramolecular H-bonding but with the H atom more strictly bound to the P=O oxygen takes place in the less stable structure **II** (O–H···N–C dihedral angle: 9.5°; H···N distance: 1.86 Å). Protonation at one of the OH centers of **1** leads to the formation of the least stable intermediate **III**, characterized by a long P···OH_2 distance (2.01 Å). Its P–C–N angle (91.8°), highly

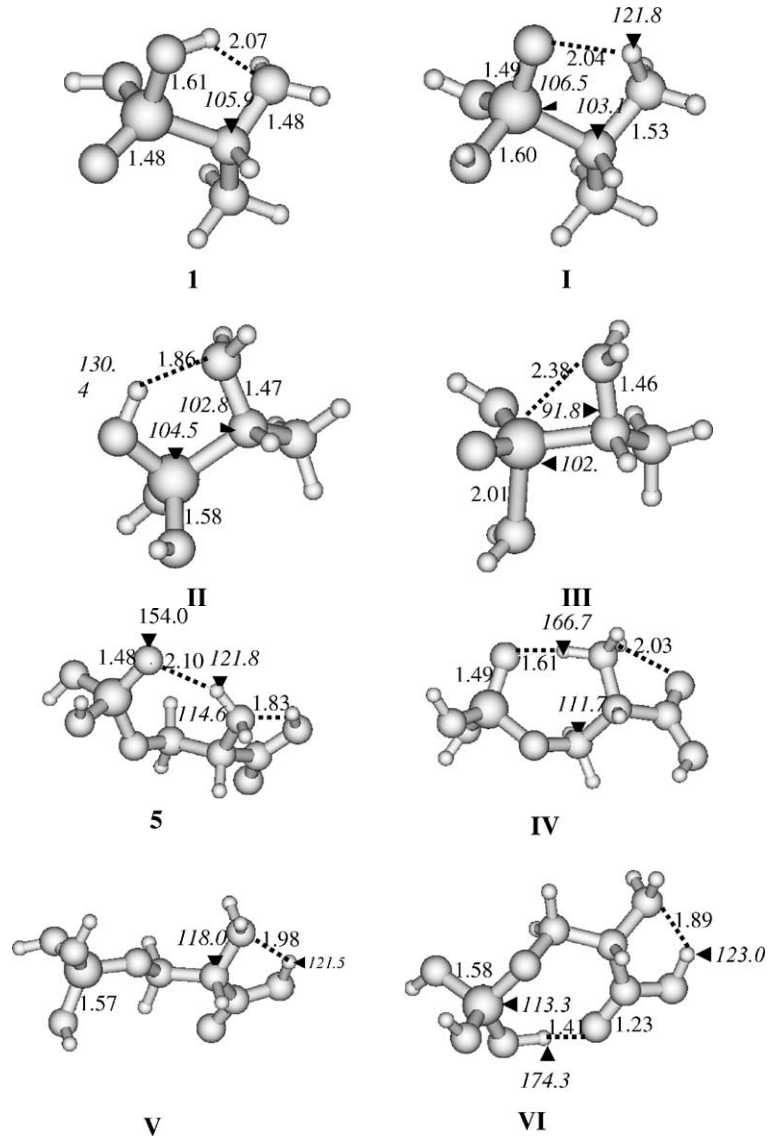

Fig. 1. B3LYP/6-31G*-optimized structures and main geometrical parameters of **1** and **5** and their protonated forms (the figure in italics above the black arrow denotes the angle in (°) centered on the signed atom; bond lengths in angstrom (Å)).

distorted relative to that of **1** (P–C–N 105.9°), suggest the backside assistance of the basic amino group of **III** to the pronounced P···OH_2 bond elongation. Adding the thermal contribution (298 K) to the total energies reported in Table 1, the proton affinity at the most basic N center of **1** amounts to 219.7 kcal mol^{-1}, while that at the P=O oxygen is calculated as large as 213.6 kcal mol^{-1}. The proton affinity at the P–OH oxygen of **1** is significantly lower (182.1 kcal mol^{-1}).

The situation is quite similar for protonated **5**, but with some important differences. Indeed, ion **IV**, formally obtained by protonating the nitrogen atom of **5**, is the global minimum on the relevant PES. Its optimized structure is characterized by some P=O···H–N

Table 1
B3LYP/6-31G*-calculated electronic energies E, 298 K enthalpies H_{298}, and proton affinities PA of **1** and **5**

Species	E (hartrees)	E (ZPV) (kcal mol^{-1})	H_{298} (hartrees)	PA (kcal mol^{-1})
1	−702.867893	74.5	−702.739459	
I	−703.229626	83.1	−703.087149	219.7
II	−703.217030	81.3	−703.077429	213.6
III	−703.166948	80.5	−703.027283	182.1
5	−966.668038	87.3	−966.515494	
IV	−967.031016	95.4	−966.865744	221.3
V	−966.995903	93.8	−966.832503	200.4
VI	−967.022601	93.5	−966.860483	218.0

coplanarity (dihedral angle: 11.0°), but now combined with a much more pronounced O···H–N colinearity (166.7° vs. 121.8° in **I**). These structural features, coupled with the very short O···H distance (1.61 Å), indicate the presence of an intense P=O···H–N electrostatic interaction in **IV**. In addition, although less intense, a H-bonding operates in **IV** between the C=O oxygen and the protonated amino group, as shown by the marked C=O···H–N flattening (dihedral angle: 14.0°) and the limited C=O···H–N distance (2.03 Å). A less stable structure **V** was recovered on the relevant PES when the proton is located on the P=O oxygen of **5**. In it, only the C–O–H···N interaction is present. A second conformer of **V** can be located on protonated **5**'s PES, i.e., structure **VI**, characterized by a pronounced O–H···O=C colinearity (174.3°) and a very short O···H distance (1.41 Å). Again, these structural features denote the presence of an intense O–H···O=C bonding in **VI**. A second H-bonding operates in **VI** between the C–O–H oxygen and the amino group, as shown by the limited O–H···N distance (1.89 Å). No stable intermediates are found by protonation at the P–O–C of **5** since the systems tend to evolve spontaneously towards structure **IV**. Protonation at one of the P–O–H oxygens of **5** induces the same kind of process which is only incipient in structure **III**, namely a ring closure with formation of a N-protonated derivative of 2-hydroxy-2-oxide-1,3,2-oxaazaphospholidine and loss of a water molecule. Two different proton affinity values can be then assigned at the P=O oxygen of **5**, one if protonation leads to the more stable conformer **VI** (PA = 218.0 kcal mol^{-1}) and the other if protonation leads to the less stable conformer **V** (PA = 200.4 kcal mol^{-1}). The highest proton affinity at the N of **5** (PA = 221.3 kcal mol^{-1}) is justified by the presence of multiple H-bonding favored by the more flexible structure of the ion, if compared to that of protonated **1** analog.

On the grounds of the above PA estimates, it is concluded that, as for the reference amino acids, the NH_2 group represents the most basic site of the selected P-containing amino acids and probably the coordination site for the relevant $[A{\cdot}H{\cdot}ref]^+$ clusters. Obviously, additional coordination between the protonation site and other basic groups, i.e., such as the vicinal PO_3H_2 or/and COOH, may take place as well. This secondary interactions may be the main reason for a nonzero difference between the entropy changes in the competitive fragmentation of Eq. (1) that must be carefully considered for a correct measurement of the PA of **1**–**7**.

3.2. Determination of the gas-phase basicities and proton affinities

Gas-phase protonation thermochemistry of **1**–**7** was evaluated from CID competitive fragmentation of the relevant proton-bound dimers $[A{\cdot}H{\cdot}ref]^+$ using the following amino acids as the reference bases: alanine (PA = 215.5 kcal mol^{-1}) [28], valine (PA = 218.1 kcal mol^{-1}) [29], leucine (PA = 218.6 kcal mol^{-1}) [28], and isoleucine (PA = 219.3 kcal mol^{-1}) [28], for the amino phosphonic

acids **1**–**4**, and aspartic acid (PA = 217.2 kcal mol^{-1}) [28], asparagine (PA = 222.0 kcal mol^{-1}) [28], glutamic acid (PA = 222.3 kcal mol^{-1}) [29], and glutamine (PA = 224.1 kcal mol^{-1}) [28] for the *O*-phospho amino acids **5**–**7**.

Fig. 2a reports a typical plot of ln([AH]$^+$/(Href]$^+$), obtained from the CID of [A·H·ref]$^+$, vs. the PA(ref) − PA(avg), where PA(avg) is the average proton affinity of the reference bases used in the determination. Similar plots were obtained for the other P-containing amino acids. In order to determine independently PA(A) and Δ(Δ*S*), i.e., the average difference between the protonation entropy of A and that of ref, the CID experiments were performed at different collision energies, corresponding to different T_{eff} values. Indeed, according to the extended treatment of the kinetic method [12], regression analysis of each set of data of Fig. 2a leads to best-fit lines whose slope m_1 corresponds to $-1/RT_{eff}$. The *y*-intercept q_1 of the best-fit lines corresponds to $\{[PA(A) - PA(avg)]/RT_{eff}\} - \Delta(\Delta S)/R$. The *x*-intercepts of the best-fit lines correspond to the relevant ΔGB(app) = GB(avg) − GB(A) difference, wherefrom the apparent proton affinity values (PA(app) = ΔGB(app) + PA(avg)) can be inferred if the entropy effects are ignored.[1]

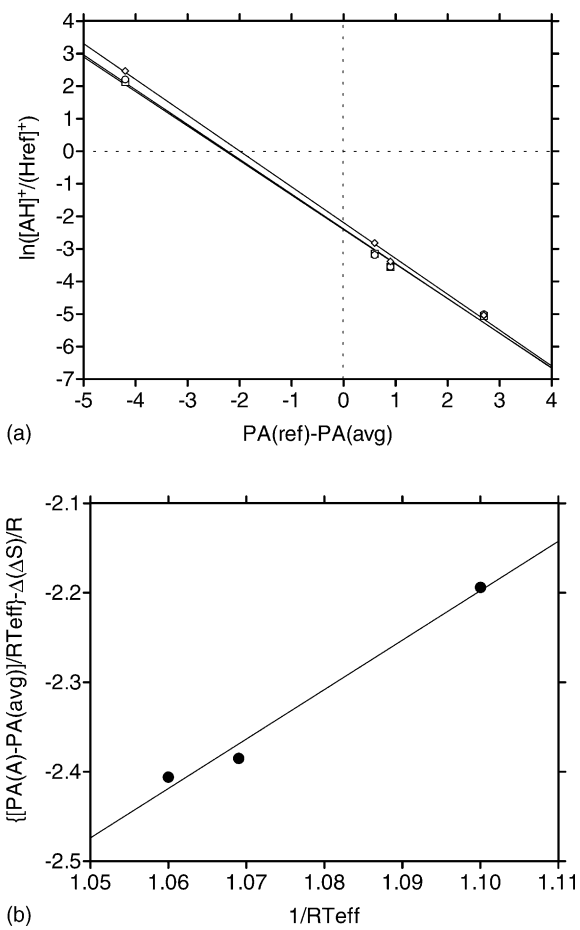

Fig. 2. (a) Plot of ln([AH]$^+$/[Href]$^+$) (A = **7**) vs. PA(ref) − PA(avg) at three different collision energies: 6 eV (diamonds); 8 eV (circles); 10 eV (squares); (b) Plot of $\{[PA(A) - PA(avg)]/RT_{eff}\} - \Delta(\Delta S)/R$ vs. $1/RT_{eff}$ for A = **7**.

A second correlation of the obtained q_1 values vs. the negative of the corresponding m_1 slopes, derived at different collision energies, gives again a straight line with a slope m_2 corresponding to PA(A) − PA(avg) and a *y*-intercept q_2 corresponding to $-\Delta(\Delta S)/R$ (Fig. 2b).[2]

The effective PA(A) values obtained for all the selected P-containing amino acids are reported in Table 2, together with the corresponding average apparent values (PA(app)), the T_{eff} terms, and the average Δ(Δ*S*) differences. A confirmation of the actual chelating properties of **1**–**7** towards the proton arises from the agreement between the B3LYP/6-31G*-calculated proton affinity of **1** and **5** and the relevant experimental values within the combined uncertainty range (±3 kcal mol^{-1}). An additional symptom of the stronger P=O···H–N intramolecular interaction in protonated **1**–**7**, relative to the analogous C=O···H–N one involved in the protonated ref, appears through the positive values of the apparent Δ(Δ*S*) differences of Table 2. The comparatively more effective chelating

[1] The recommended PA values from the compilation [28] were used for all the reference amino acids, except for glutamic acid, whose recommended PA value is 218.2 kcal mol^{-1}. Based on our measured CID fragmentation ratios, the PA of glutamic acid should be very close to that of asparagine (PA = 222.0 kcal mol^{-1}). We therefore used the value of Bojsen and Breindahl of 222.3 kcal mol^{-1} [29] for the PA of glutamic acid.

[2] The final uncertainty for the proton affinity is determined from the root sum square of the uncertainties in the slope of the plot in Fig. 2b and the uncertainty in the average proton affinity of the reference base set (see [12]).

Table 2
Protonation thermochemistry[a]

A	T_{eff} (K)				PA(app) (kcal mol^{-1})	PA(A) (kcal mol^{-1})	PA(calc) (kcal mol^{-1})	$\Delta(\Delta S)$ (cal K^{-1} mol^{-1})
	4 eV	6 eV	8 eV	10 eV				
1	$398 \pm {}^{23}_{21}$	$405 \pm {}^{17}_{16}$	$421 \pm {}^{25}_{22}$		216.1 ± 1.6	216.9 ± 1.7	219.7	+1.9 ± 0.9
2	$357 \pm {}^{27}_{22}$	$429 \pm {}^{34}_{29}$	$473 \pm {}^{31}_{27}$		217.6 ± 1.6	218.7 ± 1.6		+2.7 ± 0.4
3	$486 \pm {}^{85}_{63}$	$495 \pm {}^{109}_{75}$	$508 \pm {}^{194}_{45}$		219.0 ± 1.6	218.6 ± 1.6		−1.2 ± 0.1
4	$428 \pm {}^{39}_{33}$	$406 \pm {}^{33}_{28}$	$454 \pm {}^{39}_{34}$		218.9 ± 1.6	219.2 ± 1.8		+0.8 ± 1.8
5		$415 \pm {}^{45}_{37}$	$424 \pm {}^{37}_{32}$	$457 \pm {}^{35}_{30}$	221.6 ± 1.6	224.2 ± 1.8	221.3	+6.2 ± 1.7
6		$292 \pm {}^{54}_{40}$	$303 \pm {}^{64}_{46}$	$308 \pm {}^{76}_{51}$	221.5 ± 1.6	224.8 ± 1.7		+10.8 ± 2.7
7		$458 \pm {}^{15}_{14}$	$471 \pm {}^{25}_{21}$	$475 \pm {}^{21}_{18}$	219.2 ± 1.7	226.9 ± 1.8		+16.4 ± 1.4

[a] All uncertainties are given as 90% confidence limits.

properties of the phosphorylated amino acids **1**–**7** are responsible of the appreciable deviation between their actual PA(A) values and the corresponding apparent terms of Table 2 (PA(app)).

3.3. Chiral discrimination

The kinetic methods can be also conveniently employed to enantiodiscriminate chiral molecules, including amino acids and peptides [17,30–37]. Chiral discrimination of the (*R*)- (A_R) and (*S*)-enantiomers (A_S) of **1**–**7** is obtained by measuring the relative stability of their diastereomeric complexes with a reference amino acid of defined configuration (ref*), i.e., $[A_S{\cdot}H{\cdot}ref^*]^+$ and $[A_R{\cdot}H{\cdot}ref^*]^+$. CID of the diastereomeric proton-bound trimers $[A_S{\cdot}H{\cdot}(ref^*)_2]^+$ and $[A_R{\cdot}H{\cdot}(ref^*)_2]^+$ produces different fragmentation patterns reflecting the relevant $[A_S{\cdot}H{\cdot}ref^*]^+$ (and $[A_R{\cdot}H{\cdot}ref^*]^+$) vs. $[H{\cdot}(ref^*)_2]^+$ stability. It is convenient to define the proton-bound clusters as "homo" when A and ref* have the same configuration, and "hetero" in the opposite case. Measurement of the "homo" vs. "hetero" ion abundance ratios provides the chiral selectivity R_{chiral}, i.e.:

$$R_{chiral} = \frac{R_{homo}}{R_{hetero}} = \frac{[A_S \cdot H \cdot ref^*]^+/[H \cdot (ref^*)_2]^+}{[A_R \cdot H \cdot ref^*]^+/[H \cdot (ref^*)_2]^+} = \frac{[A_S \cdot H \cdot ref^*]^+}{[A_R \cdot H \cdot ref^*]^+} \quad (3a)$$

$$R_{chiral} = \frac{R_{homo}}{R_{hetero}} = \frac{[A_R \cdot H \cdot ref^*]^+/[H \cdot (ref^*)_2]^+}{[A_S \cdot H \cdot ref^*]^+/[H \cdot (ref^*)_2]^+} = \frac{[A_R \cdot H \cdot ref^*]^+}{[A_S \cdot H \cdot ref^*]^+} \quad (3b)$$

which is represented by Eq. (3a) if the (*S*)-enantiomer of ref* is employed and by Eq. (3b) if the (*R*)-enantiomer of ref* is used instead. In this frame, a $R_{chiral} < 1$ value indicates that the heterochiral proton-bound dimer is more stable than the homochiral analogue. The reverse is true if $R_{chiral} > 1$. If $R_{chiral} = 1$, there is no stability difference and chiral discrimination is unattainable by this method.

As an example, the CID fragmentation spectra of diastereomeric $[A_S{\cdot}H{\cdot}(ref^*)_2]^+$ and $[A_R{\cdot}H{\cdot}(ref^*)_2]^+$ complexes with A_S = (*S*)-**1**, A_R = (*R*)-**1**, and ref* = (*R*)-**4** spectrum, obtained from electrospraying their equimolar mixture in 50:50 water/methanol solutions, are reported in Fig. 3. The fragmentation patterns were found to be rather insensitive to the collision gas (N_2) pressure (5–15 mbar)) and moderately sensitive to the collision energy (4–14 eV lab frame). The reproducibility of the method was investigated by changing the chirality of ref*.

Table 3 reports the chiral resolution factors R_{chiral} for most of the selected aminophosphonic acids and the phosphorylated α-amino acids. The pronounced chelating properties of these substrates makes necessary the use of the pure enantiomers of the same

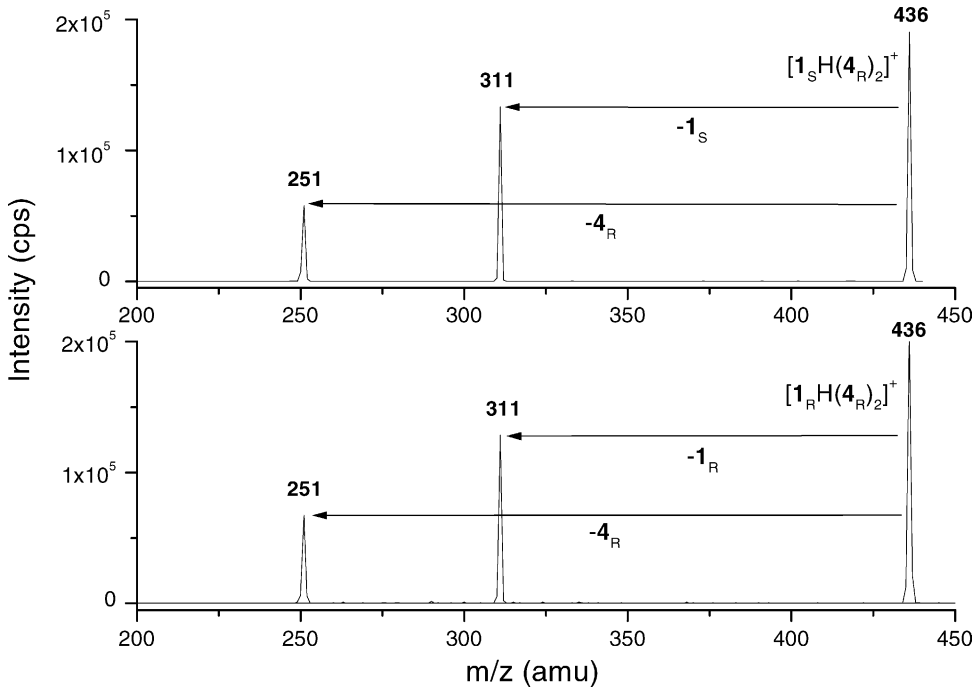

Fig. 3. CID-MS^2 spectra of diastereomeric $[A_S{\cdot}H{\cdot}(ref^*)_2]^+$ and $[A_R{\cdot}H{\cdot}(ref^*)_2]^+$ complexes (A_S = (*S*)-**1**, A_R = (*R*)-**1**, and ref* = (*R*)-**4**), using a triple quadrupole (QqQ; collision energy: 8 eV, lab frame).

substrates as ref*. Indeed, any attempt to employ the closest structural and functional analogues of A, i.e., the pure enantiomers of the α-amino acids, as the reference molecules ref* invariably failed since CID of the relevant proton-bound trimers yields invariably the $[A_S{\cdot}H{\cdot}ref^*]^+$ (or $[A_R{\cdot}H{\cdot}ref^*]^+$) fragment with the corresponding $[H{\cdot}(ref^*)_2]^+$ one below the detection limit (<0.1%).

Although the average R_{chiral} values do not appear particularly large, the accuracy and the sensitivity of the MS/MS approach are high enough to establish a stability order between the diastereomeric $[A_S{\cdot}H{\cdot}ref^*]^+$ and $[A_R{\cdot}H{\cdot}ref^*]^+$ complexes (Although qualitatively similar, the data reported in entries i–iii slightly diverges from those reported in [18] affected by a systematic error. The data in entries

Table 3
Chiral recognition of some α-amino phosphonic acids and *O*-phosphorylated amino acids

Entry	A	ref*	Chiral selectivity, R_{chiral}	Average value	Stability order
i	**1**	(*S*)-**3**	0.97	0.97 ± 0.05	hetero ≥ homo
ii	**1**	(*R*)-**3**	0.98	0.97 ± 0.05	hetero ≥ homo
iii	**3**	(*S*)-**1**	0.94	0.92 ± 0.05	hetero > homo
iv	**3**	(*R*)-**1**	0.91	0.92 ± 0.05	hetero > homo
v	**3**	(*S*)-**4**	1.00	1.00 ± 0.08	hetero = homo
vi	**4**	(*S*)-**3**	1.00	1.00 ± 0.08	hetero = homo
vii	**1**	(*S*)-**4**	1.09	1.08 ± 0.05	homo > hetero
viii	**1**	(*R*)-**4**	1.07	1.08 ± 0.05	homo > hetero
ix	**5**	(*S*)-**1**	0.84	0.85 ± 0.09	hetero > homo
x	**5**	(*R*)-**1**	0.87	0.85 ± 0.09	hetero > homo
xi	**5**	(*S*)-**6**	0.88	0.88 ± 0.11	hetero > homo

ix–xi have been taken from [38].). Proton-bound dimers of *O*-phospho α-amino acids **5** and **6** exhibit an appreciable stability difference with the heterochiral complex more stable than the homochiral one. The stability trend for the proton-bound dimers of α-aminophosphonic acids **1**, **3**, and **4** is less evident and it is found to depend critically upon their structural features. Thus, when both A and ref have the largest *R* groups (**3** and **4** of Plate 1), no chiral discrimination is observed. On the contrary, some stability differences can be appreciated when the side-chain *R* groups of A and ref have a different bulkiness, i.e., when R = CH_3 and i–C_3H_7 (entries i–iv of Table 3). Finally, it should be noted that the stability order seems sensitive to the degree of side-chain branching in A and ref (cf. entries vii and viii with entries iii and iv of Table 3).[3]

4. Conclusions

The present study highlights the successful application of the standard and extended versions of the kinetic method to the accurate measurement of the proton affinity of important residues from post-translationally modified proteins, i.e., the *O*-phospho α-amino acids, and some α-amino acid mimics, such as the chiral α-aminophosphonic acids, and to the evaluation of the differences in their protonation entropies. The kinetic method is also used to enantiodiscriminate the two enantiomers of these chiral compounds and to assess the relative stability of their proton-bound dimeric complexes.

Acknowledgements

This work was supported by the Ministero dell'Istruzione e della Ricerca (MIUR) and Consiglio Nazionale delle Ricerche (CNR): P.F. MSTAII.

[3] Another rationale for the stability order inversion in these systems can be found in the different T_{eff} for the relevant CID fragmentations. The same effect may be responsible of the slightly different average R_{chiral} values measured in the two pair of experiments of entries i/ii and iii/iv in Table 3.

References

[1] V.P. Kuhlar, H.R. Hudson (Eds.), Aminophosphonic and Aminophosphinic Acids. Chemistry and Biological Activity, Wiley, Chichester, 2000.
[2] P. Cohen, Trends Biochem. Sci. 17 (1992) 408.
[3] T. Hunter, Methods Enzymol. 200 (1991) 3.
[4] M.J. Hubbard, P. Cohen, Trends Biochem. Sci. 18 (1993) 172.
[5] T. Hunter, B. Sefton, Proc. Natl. Acad. Sci. U.S.A. 77 (1980) 1311.
[6] J.B. Fenn, N. Mann, C.K. Meng, S.F. Wong, Mass Spectrom. Rev. 9 (1990) 37.
[7] K.L. Busch, G.L. Glish, S.A. McLuckey, Mass Spectrometry/Mass Spectrometry: Techniques and Applications of Tandem Mass Spectrometry, VCH Publishers, New York, 1988.
[8] R.G. Cooks, T.L. Kruger, J. Am. Chem. Soc. 99 (1977) 1279.
[9] S.A. McLuckey, D. Cameron, R.G. Cooks, J. Am. Chem. Soc. 103 (1981) 1313.
[10] R.G. Cooks, J.S. Patrick, T. Kotiaho, S.A. McLuckey, Mass Spectrom. Rev. 13 (1994) 287.
[11] R.G. Cooks, J.T. Koskinen, P.D. Thomas, J. Mass Spectrom. 34 (1999) 85.
[12] P.B. Armentrout, J. Am. Soc. Mass Spectrom. 11 (2000) 371.
[13] A. Filippi, A. Giardini, S. Piccirillo, M. Speranza, Int. J. Mass Spectrom. 198 (2000) 137.
[14] W.Y. Shen, P.S.H. Wong, R.G. Cooks, Rapid Commun. Mass Spectrom. 11 (1997) 71.
[15] W.A. Tao, D. Zhang, F. Wang, P. Thomas, R.G. Cooks, Anal. Chem. 71 (1999) 4427.
[16] W.A. Tao, L. Wu, R.G. Cooks, J. Med. Chem. 44 (2001) 3541.
[17] K. Vékey, G. Czira, Anal. Chem. 69 (1997) 1700.
[18] A. Paladini, C. Calcagni, T. Di Palma, M. Speranza, A. Laganà, G. Fago, A. Filippi, M. Satta, A. Giardini Guidoni, Chirality 13 (2001) 707.
[19] T.T. Dang, S.F. Pedersen, J.A. Leary, J. Am. Soc. Mass Spectrom. 5 (1994) 452.
[20] X.H. Cheng, Z.C. Wu, C. Fenselau, J. Am. Chem. Soc. 115 (1993) 4844.
[21] B.A. Cerda, C. Wesdemiotis, J. Am. Chem. Soc. 118 (1996) 11884.
[22] M.J. Nold, B.A. Cerda, C. Wesdemiotis, J. Am. Soc. Mass Spectrom. 10 (1999) 1;
J. Laskin, J.H. Futrell, J. Phys. Chem. 104 (2000) 8829.
[23] A.F. Kuntz, A.W. Boynton, G.A. David, K.E. Colyer, J.C. Poutsma, J. Am. Soc. Mass Spectrom. 13 (2002) 72.
[24] J.L. Holmes, Organ. Mass Spectrom. 20 (1985) 169.
[25] M.J. Frish, G.W. Trucks, H.B. Schlegel, G.E. Scuseria, M.A. Robb, J.R. Cheeseman, V.G. Zakrzewski, J.A. Montgomery Jr., R.E. Stratman, J.C. Burant, S. Dapprich, J.M. Millam, A.D. Daniels, K.N. Kudin, M.C. Strain, O. Farkas, J. Tomasi, V. Barone, M. Cossi, R. Cammi, B. Mennucci, C. Pomelli, C. Adamo, S. Clifford, J. Ochterski, G.A. Petersson, P.Y. Ayala, Q. Cui, K. Morokuma, D.K. Malik, A.D. Rabuck, K. Raghavachari, J.B. Foresman, J. Cioslowski, J.V. Ortiz, A.G. Raboul, B.B. Stefaniv, G. Liu, A. Liashenko, P. Piskorz, I. Nanayakkara, C. Gonzales, M. Challacombe,

P.M.W. Gill, B. Johnson, W. Chen, M.W. Wong, J.L. Andres, C. Gonzales, M. Head-Gordon, E.S. Replogle, J.A. Pople, Gaussian 98, Revision A7, Gaussian, Inc., Pittsburg, PA, 1998.
[26] (a) A.D. Becke, J. Chem. Phys. 98 (1993) 1372;
(b) C. Lee, W. Yang, R.G. Parr, Phys. Rev. B 37 (1988) 785.
[27] A.P. Scott, L. Radom, J. Phys. Chem. 100 (1996) 16502.
[28] http://webbook.nist.gov/chemistry/name-ser.html.
[29] G. Bojesen, T. Breindahl, J. Chem. Soc. Perkin 2 (1994) 1029.
[30] A. Filippi, A. Giardini, S. Piccirillo, M. Speranza, Int. J. Mass Spectrom. 198 (2000) 137, and references therein.
[31] W.A. Tao, D. Zhang, E.N. Nikolaev, R.G. Cooks, J. Am. Chem. Soc. 122 (2000) 10598.
[32] W.A. Tao, L. Wu, R.G. Cooks, J. Am. Soc. Mass Spectrom. 12 (2001) 490.
[33] D. Zhang, W.A. Tao, R.G. Cooks, Int. J. Mass Spectrom. 204 (2001) 159.
[34] W.A. Tao, R.G. Cooks, Angew. Chem., Int. Ed. Engl. 40 (2001) 757.
[35] W.A. Tao, F.C. Gozzo, R.G. Cooks, Anal. Chem. 73 (2001) 1692.
[36] J. Chen, C.J. Zhu, Y. Chen, Y.F. Zhao, Rapid Commun. Mass Spectrom. 16 (2002) 1251.
[37] D.V. Augusti, R. Augusti, F. Carazza, R.G. Cooks, J. Chem. Soc., Chem. Commun. (2002) 2242.
[38] G. Fago, A. Filippi, A. Giardini, A. Laganà, A. Paladini, M. Speranza, Angew. Chem., Int. Ed. Engl. 40 (2001) 4051.